Journal of Nuclear and Radiochemical Sciences, Vol. 4, No. 1, pp. R1-R13, 2003

Reviews

Synthesis and Properties of Superheavy Elements

S. Hofmann*

Gesellschaft für Schwerionenforschung (GSI), D-64291 Darmstadt, Germany

Received: April 3, 2003

The nuclear shell model predicts that the next doubly magic shell-closure beyond ^{208}Pb is at a proton number Z = 114, 120, or 126 and at a neutron number N = 172 or 184. The outstanding aim of experimental investigations is the exploration of this region of spherical 'SuperHeavy Elements' (SHEs). Experimental methods are described which allowed for the identification of elements 107 to 112 in studies of cold fusion reactions based on lead and bismuth targets. Also presented are data which were obtained on the synthesis of elements 112, 114, and 116 in investigation of hot fusion reactions using actinide targets. The decay data reveal that for the heaviest elements, the dominant decay mode is alpha emission, not fission. Decay properties as well as reaction cross-sections are compared with the results of theoretical studies. Finally, plans are presented for the further development of the experimental set-up and the application of new techniques. At a higher sensitivity, the exploration of the region of spherical SHEs now seems to become feasible, more than thirty years after its prediction.

1. Introduction

Searching for new chemical elements is an attempt to answer questions of partly fundamental character: How many elements may exist? How long is their lifetime? Which properties determine their stability? How can they be synthesized? What are their chemical properties? How are the electrons arranged in the strong electric field of the nucleus?

Searching for new elements beyond uranium by the process of neutron capture and succeeding β^- decay, Hahn and Straßmann[1] discovered the possibility that a heavy nucleus might "divide itself into two nuclei." This was the correct interpretation given by Meitner and Frisch,[2] and the term "fission" was coined for this process. By applying the existing charged liquid-drop model of the nucleus,[3, 4] nuclear fission was explained quite naturally, and it was shown that fission will most likely limit the number of chemical elements. At that time, the maximum number of elements was expected to be about 100. This number results from the balance of two fundamental nuclear parameters, the strength of the attractive nuclear force which binds neutrons and protons together and creates a surface tension and the repulsive electric force.

The properties of nuclei are not smooth uniform functions of the proton and neutron numbers, but show non-uniformities as evidenced by variations in the measured atomic masses. Like the electrons in an atom, also the nucleons in a nucleus - described by quantum mechanical laws - form closed shells called "magic" numbers. At the magic proton or neutron numbers 2, 8, 20, 28, 50, and 82, the nuclei have an increased binding energy relative to the average trend. For neutrons, N = 126 is also identified as a magic number. However, the highest stability is observed in the case of the "doubly magic" nuclei with a closed shell for both protons and neutrons. Amongst other special properties, the doubly magic nuclei are spherical and resist deformation.

The magic numbers were successfully explained by the nuclear shell model,[5, 6] and an extrapolation into unknown regions was reasonable. The numbers 126 for the protons and 184 for the neutrons were predicted to be the next shell closures. Instead of 126 for the protons also 114 or 120 were calculated as closed shells. The term superheavy elements (SHEs) was coined for these elements.

The prediction of magic numbers, although not unambiguous, was less problematic than the calculation of the stability of those doubly closed shell nuclei against fission. As a consequence, predicted half-lives based on various calculations differed by many orders of magnitude.[7–12] Some of the half-lives approached the age of the universe, and attempts have been made to discover naturally occurring SHEs.[13, 14] Although discoveries were announced from time to time, none could be substantiated after more detailed inspection.

There was also great uncertainty of the production yields for SHEs. Closely related to the fission probability of SHEs in the ground-state, the survival of the compound nuclei formed after complete fusion was difficult to predict. Even the best choice of the reaction mechanism, fusion or transfer of nucleons, was critically debated. However, as soon as experiments could be performed without technical limitations, it turned out that the most successful methods for the laboratory synthesis of heavy elements are fusion-evaporation reactions using heavy-element targets, recoil-separation techniques, and the identification of the nuclei by generic ties to known daughter decays after implantation into position-sensitive detectors.[15–17] An overview of various methods developed for the synthesis of transuranium elements and a review of their discoveries up to the most recent attempts to produce spherical SHEs is given in Reference 18.

In the following sections a detailed description is given of the set-ups of the physical experiments used for the investigation of SHEs. (The instrumentation based on chemical methods for the study of heavy elements is presented in Reference 19.) Experiments are presented, in which cold and hot fusion reactions were used for the synthesis of SHEs. These experiments resulted in the identification of elements 107 to 112 at the Gesellschaft für Schwerionenforschung (GSI) in Darmstadt, and in the recent synthesis of elements 114 and 116 at the Joint Institute for Nuclear Research (JINR) in Dubna. We also report on a search for element 118, which started in 1999 at Lawrence Berkeley National Laboratory (LBNL) in Berkeley. In subsequent sections a theoretical description follows discussing properties of nuclei in the region of SHEs and

*Corresponding author. E-mail: s.hofmann@gsi.de. FAX: +49-6159-71-2902.

Published on Web 05/27/2003

phenomena, which influence the yield for the synthesis of SHEs. Empirical descriptions of hot and cold fusion nuclear reaction systematic are outlined. Finally, a summary and outlook is given.

2. Experimental Techniques

2.1. Targets and Accelerators. First attempts to synthesize transuranium elements based on the idea to produce β^- decaying nuclei by neutron capture, which decay into the next heavier so far unknown element. Up to fermium, this method made it possible to climb up the Periodic Table element by element. While from neptunium to californium, some isotopes can be produced in amounts of kilograms or at least grams in high neutron flux reactors, the two heaviest species, ^{254}Es and ^{257}Fm, are available only in quantities of micrograms and picograms, respectively. At fermium, however, the method ends due to the lack of β^- decay and too short α and fission half-lives of the heavier elements. Sufficiently thick enough targets cannot be manufactured from these elements.

The region beyond fermium is best accessible using heavy-ion fusion reactions, the bombardment of heavy-element targets with heavy ions from an accelerator. The cross-section is less than in the case of neutron capture and values are considerably below the geometrical size of the nuclei. Moreover, only thin targets of the order of 1 mg/cm^2 can be used. This limitation arises from the energy loss of the ion beam in the target, which results (using thicker targets) in an energy distribution that is too wide for both the production of fusion products and their in-flight separation. On the other hand, the use of thin targets in combination with well defined beam energies from accelerators results in unique information about the reaction mechanism. The data are obtained by measuring excitation functions, the yield as a function of the beam energy.

Various combinations of projectiles and targets are in principle possible for the synthesis of heavy elements: actinide targets irradiated by light projectiles of elements in the range from neon to calcium, targets of lead and bismuth irradiated by projectiles from calcium to krypton, and symmetric combinations like tin plus tin up to samarium plus samarium. Also inverse reactions using e.g. lead or uranium as projectile are possible and may have technical advantages in specific cases.

Historically, the first accelerators used for the production of heavy elements were the cyclotrons in Berkeley, California, and later in Dubna, Russia. They were only able to accelerate light ions up to about neon with sufficient intensity and up to an energy high enough for fusion reactions. Larger and more powerful cyclotrons were built in Dubna for the investigation of reactions using projectiles near calcium. These were the U300 and U400, 300 and 400 cm diameter cyclotrons. In Berkeley a linear accelerator HILAC (Heavy Ion Linear ACcelerator), later upgraded to the SuperHILAC, was built. The shutdown of this accelerator in 1992 led to a revival of heavy element experiments at the 88-Inch Cyclotron. Aiming at the acceleration of ions as heavy as uranium, the UNILAC (UNIversal Linear ACcelerator) was constructed in Darmstadt, Germany, during the years 1969–74.

In order to compensate for the decreasing cross-sections of the synthesis of heavy elements, increasing beam currents are needed from the accelerators. This demands a continuous development of ion sources in order to deliver high currents at high ionic charge states. Beam currents up to a few particle microamperes (1 μA_{part} = 6.24 × 10^{12} particles/s) are presently reached. Such high currents, in turn, demand a higher resistance of the targets. An efficient target cooling and chemical compounds with higher melting points are presently tested. The developments in the laboratories in Berkeley, Dubna, and also in Finland, France, and Italy are similar and usually made in close collaboration and exchange of know-how. Especially great progress towards the synthesis of new elements was reported recently from experiments performed at the Institute of Physical and Chemical Research (RIKEN), in Wako, Saitama, Japan (see sect. 3.1).

2.2 Recoil-Separation Techniques and Detectors. The identification of the first transuranium elements was by chemical means. In the early 1960s physical techniques were developed which allowed for detection of nuclei with lifetimes of less than one second at high sensitivity. A further improvement of the physical methods was obtained with the development of recoil separators and large area position sensitive detectors. As a prime example for such instruments, we will describe the velocity filter SHIP (Separator for Heavy-Ion reaction Products) and its detector system, which were developed at the UNILAC. The principle of separation and detection techniques used in the other laboratories is comparable.

In contrast to the recoil-stopping methods, as used in He-jet systems or mass separators, where ion sources are utilized, recoil-separation techniques use the ionic charge and momentum of the recoiling fusion product obtained in the reaction process. Spatial separation from the projectiles and other reaction products is achieved by combined electric and magnetic fields. The separation times are determined by the recoil velocities and the lengths of the separators. They are typically in the range of 1-2 μs. Two types of recoil separators have been developed: (1) The gas-filled separators use the different magnetic rigidities of the recoils and projectiles travelling through a low pressure (about 1 mbar) gas-filled volume in a magnetic dipole field.[20] In general, helium is used in order to obtain a maximum difference in the rigidities of slow reaction products and fast projectiles. A mean charge state of the ions is achieved by frequent collisions with the atoms of the gas. (2) Wien-filter or energy separators use the specific kinematic properties of the fusion products. The latter are created with velocities and energies different from the projectiles and other reaction products. Their ionic charge state is determined when they escape from a thin solid-state target into vacuum. Ionic-charge achromaticity is essential for high transmission. It is achieved by additional magnetic fields or symmetric arrangements of electric fields. An example of such a separator used in experiments for the investigation of heavy elements is the velocity filter SHIP in Darmstadt[15] shown in Figure 1.

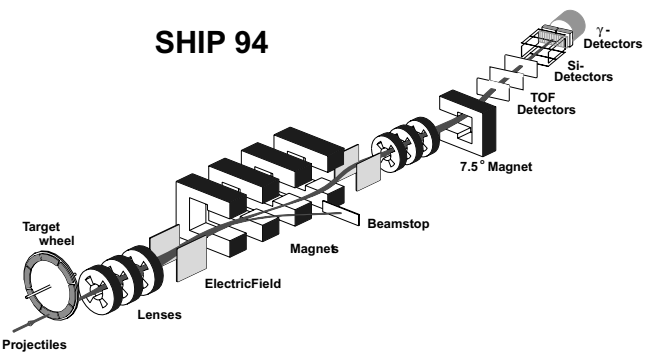

Figure 1. The velocity filter SHIP (Separator for Heavy Ion reaction Products) and its detection system.[15–17] The drawing is approximately to scale, however, the target wheel and the detectors are enlarged by a factor of two. The length of SHIP from the target to the detector is 11 m. The target wheel has a radius up to the center of the targets of 155 mm. It rotates synchronously with beam macrostructure at 1125 rpm.[21] The target thickness is usually 450 μg/cm^2. The detector system consists of three large area secondary-electron time-of-flight detectors[22] and a position-sensitive silicon-detector array (see text). The flight time of the reaction products through SHIP is 2 μs. The filter, consisting of two electric and four magnetic dipole fields plus two quadrupole triplets, was extended by a fifth deflection magnet, allowing for positioning of the detectors away from the straight beam line and further reduction of the background.

Recoil separators are designed to filter out those nuclei with a high transmission, which are produced in fusion reactions. Since high overall yields result in increased background levels, the transmitted particles have to be identified by detector systems. The detector type to be selected depends on the particle rate, energy, decay mode, and half-life. Experimental as well as theoretical data on the stability of heavy nuclei show that they decay by α emission, electron capture or fission, with half-lives ranging from microseconds to days. Therefore silicon semiconductor detectors are well suited for the identification of nuclei and for the measurement of their decay properties. If the total rate of ions striking the focal plane of the separator is low, then the particles can be implanted directly into the silicon detectors. Using position-sensitive detectors, one can measure the local distribution of the implanted particles. In this case, the detectors act as diagnostic elements to optimize and control the ion optical properties of the separator.

Given that the implanted nuclei are radioactive, the positions measured for the implantation and all subsequent decay processes are the same. This is the case because the recoil effects are small compared with the range of implanted nuclei, emitted α particles or fission products, and detector resolution. Recording the data event by event allows for the analysis of delayed coincidences with variable position and time windows for the identification of the decay chains.[16]

The presently used detector system is composed of three time-of-flight detectors, seven identical 16-strip silicon wafers, and germanium detectors.[17] A schematic view of the detector arrangement is shown in the focal plane of SHIP in Figure 1. Three secondary-electron foil detectors in front of the silicon detectors are used to measure the velocity of the particles.[22] They are mounted 150 mm apart from each other. The detector signals are also used to distinguish implantation from radioactive decays of previously implanted nuclei. Three detectors are used to increase the detection efficiency.

A time-of-flight signal and an energy signal from the silicon detector provide the information for switching off the beam after detection of an implanted residue.[23] After a response time of 20 μs a subsequent time window of preset duration opens for counting a preset number of α particles of the decay chain. If the desired conditions are fulfilled, the beam-off period is prolonged up to the expected measurable end of the decay chain by opening a third time window. This improvement considerably reduces the background during the measuring period of the decay chain and allows for the safe detection of signals from long lived decays. The sequence of three time windows is needed because time-of-flight and energy signals alone would trigger the switching off process for the beam too often due to background events in the corresponding windows.

3. Experimental Results

3.1. Elements Produced in Cold-Fusion Reactions. In this section, we present results dealing with the discovery of elements 107 to 112 using cold fusion reactions based on lead and bismuth targets. A detailed presentation and discussion of the decay properties of elements 107 to 109 and of elements 110 to 112 was given in previous reviews.[17, 24, 25] Known elements and their position in the Periodic Table of the Elements are shown in Figure 2. An overview of nuclei and decay chains in the region of SHEs, which are presently known or under investigation, is given in the partial chart of nuclides (Figure 3).

Bohrium, element 107, was the first new element synthesized at SHIP using the method of in-flight recoil separation and generic correlation of parent-daughter nuclei. The reaction used was $^{54}Cr + {}^{209}Bi \rightarrow {}^{263}Bh^*$. Five decay chains of ^{262}Bh were observed.[42] The next lighter isotope, ^{261}Bh, was synthesized at a higher beam energy.[43] Additional data were obtained from the α decay of ^{266}Mt,[44] and the isotope ^{264}Bh was identified as granddaughter in the decay chain of $^{272}111$.[23, 29] The isotopes ^{266}Bh and ^{267}Bh were produced using the hot fusion reaction $^{22}Ne + {}^{249}Bk \rightarrow {}^{271}Bh^*$.[39, 40] These nuclei were used for a study of the chemical properties of bohrium.

Hassium, element 108, was first synthesized in 1984 using the reaction $^{58}Fe + {}^{208}Pb$. The identification was based on the observation of three atoms.[45] Only one α-decay chain was measured in the irradiation of ^{207}Pb with ^{58}Fe. The measured event was assigned to the even-even isotope ^{264}Hs.[46] The results were confirmed in a later work,[25, 27] and for the decay of ^{264}Hs, a fission branching of 50% was also measured. The isotope ^{269}Hs was discovered as a link in the decay chain of $^{277}112$,[23, 28] and ^{270}Hs was identified in a recent chemistry experiment.[41]

Meitnerium, element 109, was first observed in the year 1982 in the irradiation of ^{209}Bi with ^{58}Fe by a single α-decay chain.[47, 48] This result was confirmed later.[49] In the most recent experiment[44] twelve atoms of ^{266}Mt have been measured, revealing a complicated decay pattern, as could be concluded from the wide range of α energies from 10.5 to 11.8 MeV. This property seems to be common to many odd and odd-odd nuclides in the region of the heavy elements. The more neutron-rich isotope ^{268}Mt was measured after α decay of $^{272}111$.[23, 29]

Element 110 was discovered in 1994 using the reaction $^{62}Ni + {}^{208}Pb \rightarrow {}^{269}110 + 1n$.[27] The main experiment was preceded by a thorough study of the excitation functions for the synthesis of ^{257}Rf and ^{265}Hs using beams of ^{50}Ti and ^{58}Fe in order to determine the optimum beam energy for the production of element 110. New information on the decay pattern of these nuclei was also obtained. The data revealed that the maximum cross-section for the synthesis of element 108 was shifted to a lower excitation energy, different from the predictions of reaction theories. An extra-push energy was not measured.

The heavier isotope $^{271}110$ was synthesized with a beam of the more neutron-rich isotope ^{64}Ni.[25] The important result for the further production of elements beyond meitnerium was that the cross-section was enhanced from 2.6 pb to 15 pb by increasing the neutron number of the projectile by two, which gave hope that the cross-sections for the synthesis of heavier

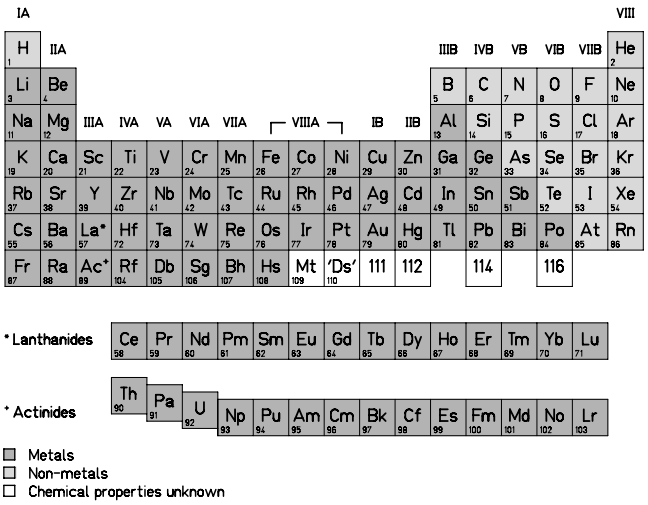

Figure 2. Periodic Table of the Elements. The known transactinide elements 104 to 116 take the positions from below Hf in group IVA to below Po in group VIB. Element 108, hassium (Hs), the heaviest element chemically investigated, is placed in group VIIIA. The arrangement of the actinides reflects the fact that the first actinide elements still resemble, to a decreasing extent, the chemistry of the other groups: Th (group IVA below Hf), Pa (group VA below Ta), and U (group VIA below W).[26] The name 'darmstadtium', symbol 'Ds' was proposed for element 110 and recommended for acceptance by the Inorganic Chemistry Division of IUPAC in February 2003.

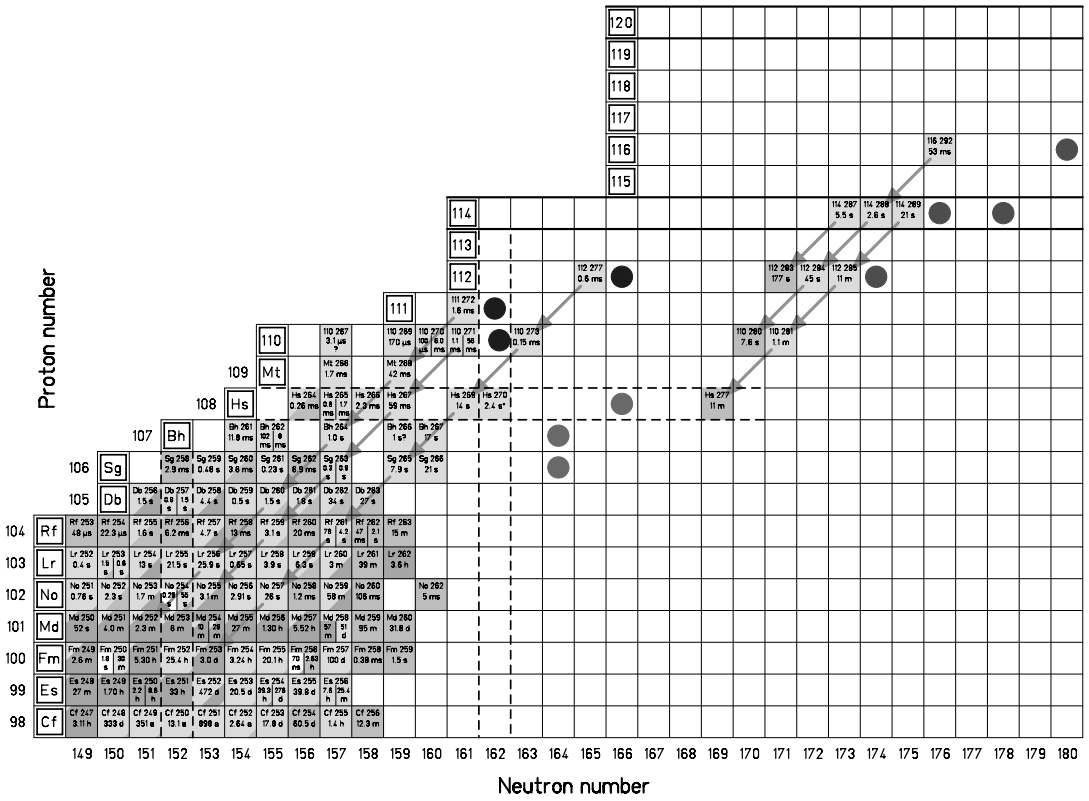

Figure 3. Upper end of the chart of nuclei showing the known nuclei and those which are presently (2003) under investigation. For each known isotope the element name, mass number, and half-life are given. The dots mark compound nuclei of reactions which were used to study the heaviest elements. In cold fusion reactions using ^{208}Pb target and beams of ^{64}Ni, ^{70}Zn for the study of elements 110 and 112 in Darmstadt.[27, 28] Element 111 was produced with a ^{64}Ni beam on a ^{209}Bi target.[23, 29] The isotopes of the new elements were identified by decay chains (nuclei connected with arrows) which ended in known, previously studied nuclei. The parent nucleus was created after evaporation of one neutron from the compound nucleus. The compound nuclei of elements 112, 114 and 116 studied in Dubna using a ^{48}Ca beam and targets of ^{238}U,[30] ^{242}Pu,[31] ^{244}Pu,[32, 33] and ^{248}Cm.[34, 35] The observed decay chains are shown together with their assignment to superheavy nuclei created after evaporation of three and four neutrons, respectively. Finally, the compound nuclei used by nuclear chemists for the study of the chemical properties of elements seaborgium (Sg),[36–38] bohrium (Bh)[39, 40] and hassium (Hs).[41] The elements were synthesized in reactions with beams of ^{22}Ne and ^{26}Mg and targets of ^{248}Cm and ^{249}Bk. Relatively long lived isotopes were produced after evaporation of four and five neutrons. The magic numbers for the protons at element 114 and 120 are emphasized. The bold dashed lines mark proton number 108 and neutron numbers 152 and 162. Nuclei with that number of protons or neutrons have increased stability, however, they are deformed contrary to the spherical superheavy nuclei. The crossing at Z = 114 and N = 162 reflects the uncertainty, whether nuclei in that region are deformed or spherical.

elements could decrease less steeply with available stable, more neutron-rich projectiles. However, this expectation was not proven in the case of element 112.

An overview of all data measured at SHIP from the decay chains observed in the reaction ^{64}Ni + ^{208}Pb $\rightarrow$ ^{272}110* is given in Figure 4. The energies and lifetimes of α decays directly succeeding the implantations are shown. (Describing single event chains it is preferable to use the lifetime τ instead of the half-life, because τ is directly measured as time difference between two succeeding signals). On top of the upper abscissa the α spectra deduced from literature are plotted for the decays of ^{255}Md, ^{255}No, ^{259}Rf, and ^{263}Sg, in order to compare the energy and intensity pattern with the measured data assigned to the decay of ^{271}110. In case of ^{267}Hs the three α decays observed by Lazarev et al.[50] are plotted.

The event chains are ordered chronologically from number 1 to 13. For each chain, the time sequence of the α decays is from right to left following the decreasing α energies. The lifetimes of the first α decays at 10.7 MeV are the time differences between implantation and α decay.

A total number of 57-α decays were measured and assigned to the 13 decay chains. Thirty-eight α's were emitted in beam direction and stopped in the 300-μm thick detector. These α events are marked by the little filled squares. The width of the squares shows the energy resolution of 13 keV (2σ) obtained for these full energy α signals. An exception are the ^{271}110 α decays of chain 9 and 11 for which the energy had to be corrected by +60 keV and –40 keV, respectively, due to short lifetime and tails of the signals from the preceding implantation. A larger error bar, as indicated by the rectangles, was used. The larger, open squares mark escape α's for which the full energy could be summed from ΔE signals between 0.6 and 1.4 MeV in the stop detector and coincident residual energies in the backward crystals. A total of 12 of these α events were measured, for which an energy resolution of 34 keV (2σ), as

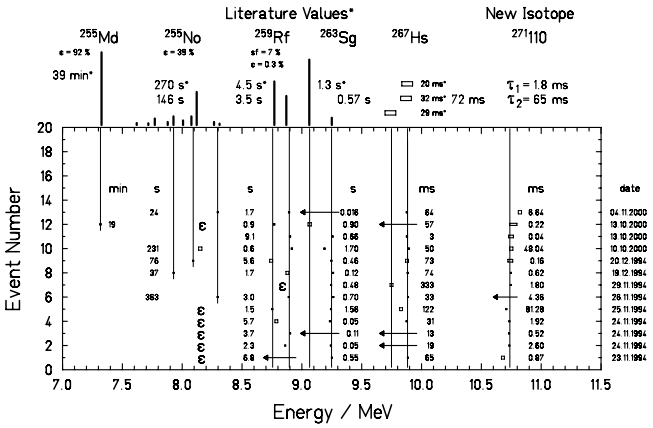

Figure 4. Energies and lifetimes of the thirteen α-decay chains resulting from the reaction ^{64}Ni + ^{208}Pb $\rightarrow$ ^{271}110 + 1n. The isotope ^{271}110 was identified by comparison of the decay properties of the daughter products with literature data marked by an asterisk (^{267}Hs,[50] ^{263}Sg,[51] ^{259}Rf,[52] ^{255}No,[52] ^{255}Md.[52]). New decay data of the isotope ^{263}Sg could be deduced. The decay chains are arranged chronologically with the date of production given at the righthand ordinate. For description of the symbols see text.

marked by the width of the squares, was obtained in test reactions at higher statistical significance. In one of these cases, chain number 12, the first α decay was corrected by +60 keV due to the short lifetime after the implantation, and a larger error bar was used. Seven α's escaped missing the backward crystals, but still leaving a ΔE signal and thus the time and position information. The amplitudes of the signals corresponded to energies between 1.0 and 5.2 MeV, which is characteristic for escaping α particles. They are marked in Figure 4 by the arrows pointing left. The ratio of the α's measured with full energy/escape plus residual energy/escape is 38/12/7. It agrees within statistical error bars with the ratio 60/30/10 determined by test reactions.

The lower discriminator level for signals in the stop detector was at 260 keV, which is below the lowest ΔE signals of escaping α's emitted from heavy nuclei implanted 4–6 μm into the active detector material. An estimate of the implantation depths was obtained by the measured implantation energy signals of ≈25 MeV. As an important result a detection efficiency for α decay of 100% was obtained, the same as for the much higher energetic fission events. In case of a missing α decay or fission signal the reason must be that the nucleus, which has been identified as an α-decay product, undergoes β decay or electron capture. In Figure 4 these missing α or fission decays are marked by "ε". If the time windows can be opened wide enough to cover the full lifetime range, the detector system allows an unambiguous measurement of β-branching ratios.

In agreement with the known branching ratios of ^{255}No (b_ε = 39%[52]) and ^{255}Md (b_α = 8%[52]) is the observation of the α decay of ^{255}Md in one of 13 cases (see chain 12 in Figure 4). This example reveals firstly that lifetimes up to 19 min are measurable at low background rate (in our case the ^{255}Md α decay occurred during a beam pause of 14.5 ms) and secondly that agreement of α energies with literature data is much more significant for the identification in the case of monoenergetic decays or simple decay patterns. The widely spread α energies of the ^{255}No decay represents an opposite example.

The decay data of the isotope ^{271}110 and its daughter products were confirmed in a recent experiment at RIKEN, where the same reaction, ^{64}Ni + ^{208}Pb → ^{272}110*, was studied and a total of 14 decay chains were measured.[53, 54] The α energy agrees well with our value of 10.74 MeV and also for the lifetime a long lived (3 events) and a short lived (11 events) components were measured. Mean values obtained from all 5 long lived and 22 short lived decays are τ = 100 ms and 2.35 ms, respectively, from which half-lives of (69^{+56}_{-21}) ms and ($1.63^{+0.44}_{-0.28}$) ms follow.

Obviously isomeric states are responsible for the two different half-lives. Because the measured α energies are almost identical, an explanation suggested by Morita et al.[53] seems very likely; the isomeric state has the longer half-life and decays dominantly by γ emission or internal conversion into the shorter lived ground-state. Both states are populated in the reaction, but because the lifetime is measured as interval between implantation and α decay, we observe two different values for one and the same α transition. Theoretically low spin and high spin states ($1/2^+$ to $13/2^-$) which could result in isomeric states close to the ground-state were predicted by Ćwiok et al.[55] The isomeric ratio between population of the 69 ms and 1.6 ms states is 5/22. Therefore we may further conclude that the relatively long lived isomeric state has a low spin value and is less populated. However, this spin dependence known from lighter nuclei may be changed for heavy systems due to reduced fission probability of the compound nucleus at high spin. Also the possibility that both levels decay by α emission with almost the same α energy cannot be completely excluded. An indication could be the slightly lower α energy in the case of chain number 5 for the longer lived decay, which was measured with high precision.

Further confirmation of the production of ^{271}110 in the reaction ^{64}Ni + ^{208}Pb → ^{272}110* was reported recently from an experiment performed at the Berkeley Gas-filled Separator (BGS).[56] At a beam energy of 309 MeV at the center of the target two decay chains were measured from which a cross-section of 8.3 pb was deduced. This value is in agreement with our result.[25] We conclude that the maximum deviation of beam energy measured at the LBNL 88-Inch Cyclotron and the UNILAC is ±2 MeV. Similar deviation is deduced from a comparison of the data measured at RIKEN[54] and at the UNILAC. Possibilities to improve the accuracy of beam-energy measurements are presently discussed.

Two more isotopes of element 110 have been reported in the literature. The first is ^{267}110, produced at LBNL in the irradiation of ^{209}Bi with ^{59}Co.[57] The second isotope is ^{273}110, reported to be observed at JINR in the irradiation of ^{244}Pu with ^{34}S after the evaporation of five neutrons.[58] Both observations need further experimental clarification.

The even-even nucleus ^{270}110 was synthesized using the reaction ^{64}Ni + ^{207}Pb.[59] A total of eight α-decay chains were measured during an irradiation time of seven days. Decay data were obtained for the ground-state and a high spin K isomer, for which calculations predict spin and parity 9^-, 10^- or 8^+.[60] The relevant single particle Nilsson levels are $\nu[613]_{7/2+}$ and $\nu[615]_{9/2+}$ below the Fermi level and $\nu[725]_{11/2-}$ above the Fermi level. Configuration and calculated energy of the excited states are $\{\nu[613]_{7/2+}\ \nu[725]_{11/2-}\}_{9-}$ at 1.31 MeV, $\{\nu[615]_{9/2+}\ \nu[725]_{11/2-}\}_{10-}$ at 1.34 MeV, and $\{\nu[613]_{7/2+}\ \nu[615]_{9/2+}\}_{8+}$ at 1.58 MeV.

The new nuclei ^{266}Hs and ^{262}Sg were identified as daughter products after α decay. Spontaneous fission of ^{262}Sg terminates the decay chain. A proposed partial decay scheme of ^{270}110 is shown in Figure 5.

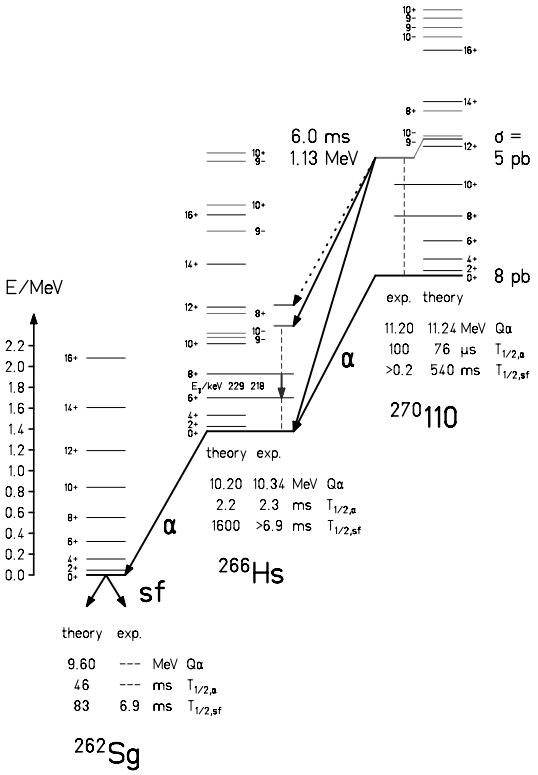

Figure 5. Tentative assignment of measured α and γ decay and spontaneous fission data observed in the reaction ^{64}Ni + ^{207}Pb → ^{271}110*. The data were assigned to the ground-state decays of the new isotopes ^{270}110, ^{266}Hs, and ^{262}Sg and to a high spin K isomer in ^{270}110. Arrows in bold represent measured α and γ rays and spontaneous fission. The proposed partial level schemes are taken from theoretical studies of Muntian et al.[61] for the rotational levels, of Ćwiok et al.[60] for the K isomers and of Smolanczuk[62] and Smolanczuk et al.[63] for the α energies and spontaneous fission half-life of ^{262}Sg, respectively. For a detailed discussion see Reference 59.

Element 111 was synthesized in 1994 using the reaction ^{64}Ni + ^{209}Bi → ^{273}111*. A total of three α chains of the isotope ^{272}111 were observed.[29] Three additional decay chains were measured in a confirmation experiment in October 2000.[23]

Element 112 was investigated at SHIP using the reaction ^{70}Zn + ^{208}Pb → ^{278}112*.[28] The irradiation was performed in January-February 1996. Over a period of 24 days, a total of 3.4×10^{18} projectiles were collected. One α-decay chain, shown in the left side of Figure 6, was observed resulting in a cross-section of 0.5 pb. The chain was assigned to the one neutron-emission channel. The experiment was repeated in May 2000 aiming to confirm the synthesis of ^{277}112.[23] During a similar measuring time, but using slightly higher beam energy, one more decay chain was observed, also shown in Figure 6. The measured decay pattern of the first four α decays is in agreement with the one observed in the first experiment.

A new result was the occurrence of fission which ended the second decay chain at ^{261}Rf. A spontaneous-fission branch of this nucleus was not yet known, however, it was expected from theoretical calculations. The new results on ^{261}Rf were proven in a recent chemistry experiment,[41] in which this isotope was measured as granddaughter in the decay chain of ^{269}Hs (see the following sect. 3.2).

A reanalysis of all decay chains measured at SHIP since 1994, a total of 34 decay chains were analyzed, revealed that the previously published[28] first decay chain of ^{277}112 (not shown in Figure 6) and the second of the originally published[27] four chains of ^{269}110 were spuriously created. Details of the results of the reanalysis are given in Reference 23.

Results from an experiment at the 88-Inch Cyclotron in Berkeley aiming to synthesize element 118 were published in 1999.[64] Using the new BGS the reaction ^{86}Kr + ^{208}Pb → ^{294}118* was investigated. From three decay chains consisting of six subsequent α decays a surprisingly high cross-section of 2 pb was deduced for the one neutron emission channel.

In order to confirm the data obtained in Berkeley, the same reaction was investigated at SHIP in the summer of 1999. The experiment is described in detail in Reference 17. During a measuring time of 24 days a beam dose of 2.9×10^{18} projectiles was collected which was comparable to the Berkeley value of 2.3×10^{18}. No event chain was detected, and the cross-section limit resulting from the SHIP experiment for the synthesis of element 118 in cold fusion reactions was 1.0 pb. Also from the laboratories GANIL in Caen, France,[65] and RIKEN[66] negative results were reported. The Berkeley data were retracted in the summer of 2001[67] after negative results of a repetition experiment performed in the year 2001 in Berkeley itself and after a reanalysis of the data of the first experiment,

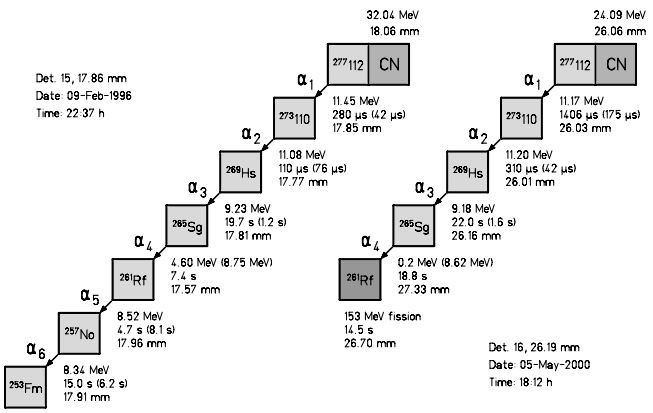

Figure 6. Two decay chains measured in experiments at SHIP in the cold fusion reaction ^{70}Zn + ^{208}Pb → ^{278}112*. The chains were assigned to the isotope ^{277}112 produced by evaporation of one neutron from the compound nucleus. The lifetimes given in brackets were calculated using the measured α energies. In the case of escaped α particles the alpha energies were determined using the measured lifetimes.

which showed that the three reported chains were not in the 1999 data. A comparison of the measured cross-section limit for this reaction with predictions from theoretical models is given in sect. 5.

3.2. Elements Produced in Hot-Fusion Reactions. Hot fusion reactions are based on targets made from actinide elements. A number of differences exist compared with reactions using lead or bismuth targets. Probably the most significant is the excitation energy of the compound nucleus at the lowest beam energies necessary to initiate a fusion reaction. Values are at 10 – 20 MeV in reactions with lead and bismuth targets and at 35 – 45 MeV in reactions with actinide targets, which led to the widely used terminology of 'cold' and 'hot' fusion reactions. Due to the lack of targets between bismuth and thorium, a gradual change from cold to hot fusion cannot be studied experimentally. A second important difference of actinide target based reactions is the synthesis of more neutron-rich isotopes compared with a cold fusion reaction leading to the same element, e.g. ^{269}Hs from a ^{248}Cm target (see below) and ^{264}Hs from a ^{208}Pb target using beams of ^{26}Mg and ^{58}Fe, respectively.

Actinides served already as targets, when neutron capture and subsequent β^- decay were used for the first synthesis of transuranium elements. Later, up to the synthesis of seaborgium,[51] actinides were irradiated with light-ion beams from accelerators. Then, cold fusion reactions were used with lead and bismuth targets, which resulted in higher yield for the synthesis of heavy nuclei.

The argumentation changed again when elements 110 to 112 had been discovered in cold fusion reactions and continuously decreasing cross-sections were measured. The combination of actinide targets with beams as heavy as ^{48}Ca became promising to study more neutron rich isotopes which are closer to the region of spherical SHEs and for which also longer half-lives were expected. In addition the lowest excitation energies of compound nuclei from fusion with actinide targets are obtained with beams of ^{48}Ca.

The experimental difficulty with using a ^{48}Ca beam is the low natural abundance of only 0.19% of this isotope, which makes enrichment very expensive. Therefore, the development of an intense ^{48}Ca beam at low consumption of material in the ion source and high transmission through the accelerator was the aim of the work accomplished in Dubna during a period of about two years until 1998.[68]

The experiments at the U400 cyclotron were performed at two different recoil separators, which had been built during the 1980s. The separators had been upgraded in order to improve the background suppression and detector efficiency. The energy-dispersive electrostatic separator VASSILISSA was equipped with an additional deflection magnet.[69, 70] The gas-filled separator GNS was tuned for the use of very asymmetric reactions with emphasis on the irradiation of highly radioactive targets.[71] Both separators were equipped with time-of-flight detectors and with an array of position-sensitive Si detectors in an arrangement similar to the one shown in Figure 1.

At the separator VASSILISSA attempts were undertaken to search for new isotopes of element 112 by irradiation of ^{238}U with ^{48}Ca ions.[30] The irradiation started in March, 1998. Two fission events were measured resulting in a cross-section of 5.0 pb. The two events were tentatively assigned to the residue ^{283}112 after 3n evaporation.

The experiments were continued in March 1999. The reaction ^{48}Ca + ^{242}Pu → ^{290}114* was investigated.[31] It was expected that, after evaporation of three neutrons, the nuclide ^{287}114 would be produced and would decay by α emission into the previously investigated ^{283}112. Over a period of 21 days, a total of four fission events were detected. Two of them could be assigned to fission isomers. The other two fission signals were preceded by signals from α particles (one was an escape

α of 2.31 MeV) and implantations. A cross-section of 2.5 pb was obtained for the two events. They were assigned to the nuclide ^{287}114. The four events, two from 112 and two from 114 of the ^{238}U and ^{242}Pu irradiation with ^{48}Ca, are consistent. The fission lifetimes are within the limits given by statistical fluctuations. Fission was measured again after α decay, when the target was changed from ^{238}U to ^{242}Pu. The low background rate in the focal plane of VASSILISSA makes mimicking by chance coincidences unlikely. However, further investigation is needed for an unambiguous assignment.

At GNS a search for element 114 was started in November-December, 1998. The experiments were performed in collaboration between the Flerov Laboratory of Nuclear Reactions (FLNR) of JINR and the Lawrence Livermore National Laboratory (LLNL), Livermore, California. A ^{244}Pu target was irradiated for a period of 34 days with a ^{48}Ca beam. One decay chain was extracted from the data. The chain was claimed to be a candidate for the decay of ^{289}114. The measured cross-section was 1 pb.[32]

The ^{48}Ca + ^{244}Pu experiment was repeated in June-October, 1999. During a period of 3.5 months, two more α-decay sequences, terminating in spontaneous fission, were observed.[33] The two chains were identical within the statistical fluctuations and detector-energy resolution, but differed from the first chain measured in 1998. The two new events were assigned to the decay of ^{288}114, the 4n evaporation channel. The cross-section was 0.5 pb.

An investigation of element 116 was started in June 2000. Using a ^{248}Cm target, the previously detected isotopes ^{289}114 or ^{288}114 were expected to be observed as daughter products from the decay of the corresponding element 116 parent nuclei produced after evaporation of 3 or 4 neutrons. The first decay chain which was assigned to ^{292}116 was measured after 35 days on July 19, 2000.[34] The irradiation was continued later, and two more decay chains were measured on May 2 and 8, 2001.[35] All three decay chains are plotted in Figure 7. The cross-section is about 0.6 pb deduced from a total beam dose of 2.25 $\times 10^{19}$.

The newly measured chains are of high significance. The data reveal internal redundancy, and the lifetimes are relatively short, making an origin by chance events extremely unlikely. In particular, because all further decays in the chain, after the parent decay was observed, were measured during a beam free period. The beam was switched off using as a trigger the time-of-flight and energy signals from the implantation and the α decay from the parent. The assignment to the 4n channel is likely, but remains subject to further investigation until an unambiguous identification will become possible. As the

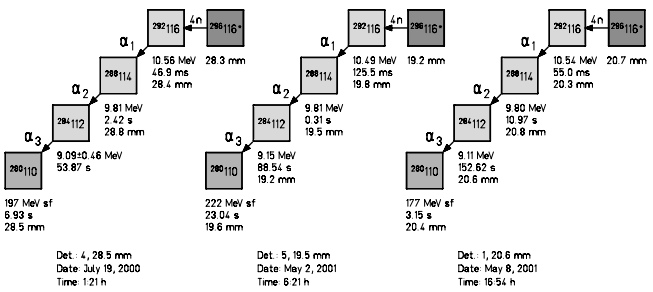

Figure 7. Three decay chains measured in the reaction ^{48}Ca + ^{248}Cm $\rightarrow$ ^{296}116* at JINR in Dubna.[35] After implantation of the evaporation residue and detection of the first α decay, the beam was switched off and the succeeding decays were measured under almost background free conditions. The decays assigned to the daughter nucleus ^{288}114 were in agreement with the data measured previously from two decay chains in the reaction ^{48}Ca + ^{244}Pu $\rightarrow$ ^{292}114*.[33] The time values given are the measured intervals between successive signals and represent the lifetimes of the decays. Also given are the measured positions in mm, where in the vertically arranged detector strips the events occurred. The figure was prepared using data given in Reference 35.

chains end at ^{280}110 by spontaneous fission, generic relations to known nuclei cannot be used. Other possible procedures which could help to establish a unique assignment, could be measurements of excitation functions, further cross bombardments, direct mass measurements, and chemical analysis of parent or daughter elements. Also a systematic investigation of the nuclei in the gap between those studied mainly at GSI and that measured in Dubna would be useful.

How well chemical properties can be used for the separation and identification of even single atoms was recently demonstrated in an experiment to study hassium.[41] Using the hot fusion reaction ^{26}Mg + ^{248}Cm $\rightarrow$ ^{274}Hs*, the isotope ^{269}Hs was produced after evaporation of five neutrons. The hassium atoms, a total of three decay chains were measured, reacted with oxygen to form the volatile compound HsO_4. This way it was proven independently by chemical means that the produced atom belongs, like osmium which also forms a volatile tetroxide, to group VIIIA and thus to element 108 in the Periodic Table of the Elements (Figure 2). The measured decay properties of the separated atoms fully confirmed the data obtained from the decay ^{277}112.[23]

Hot fusion reactions applied to synthesize long-lived nuclides of elements 104 through 108 for chemical studies are summarized in Table 1.[26] Cross-sections vary from about 10 nb to a few pb.[39–41, 72–74] With typical beam intensities of 3 $\times$ 10^{12} ions per second on targets of about 0.8 mg/cm^2 thickness production yields range from a few atoms per minute for rutherfordium and dubnium isotopes to five atoms per hour for ^{265}Sg and even less for ^{267}Bh and heavier nuclides. Therefore, all chemical separations are performed with single atoms on an "atom-at-a-time" scale. Similar to the experiments with recoil separators characteristic α decays and time correlated α-α-decay chains are used to identify these nuclides in specific fractions or at characteristic positions after chemical separation.

TABLE 1: Nuclides From Hot Fusion Reactions[26] Used in Chemical Investigations

Nuclide	$T_{1/2}$ (s)	Beam	Target	Channel	Cross-section (pb)	Yield
^{261m}Rf	78	^{18}O	^{248}Cm	5n	≈10,000	2 min^{-1}
		^{22}Ne	^{244}Pu	5n	4,000	1 min^{-1}
^{262}Db	34	^{18}O	^{249}Bk	5n	6,000	2 min^{-1}
		^{19}F	^{248}Cm	5n	1,000	0.5 min^{-1}
^{263}Db	27	^{18}O	^{249}Bk	4n	10,000	3 min^{-1}
^{265}Sg	7.4	^{22}Ne	^{248}Cm	5n	≈240	5 h^{-1}
^{266}Sg	21	^{22}Ne	^{248}Cm	4n	≈25	0.5 h^{-1}
^{267}Bh	17	^{22}Ne	^{249}Bk	5n	≈70	1.5 h^{-1}
^{269}Hs	14	^{26}Mg	^{248}Cm	5n	≈6	3 d^{-1}
^{270}Hs	2-7	^{26}Mg	^{248}Cm	4n	4	2 d^{-1}

4. Nuclear Structure and Decay Properties

The calculation of the ground-state binding energy provides the basic step to determine the stability of SHEs. In macroscopic-microscopic models the binding energy is calculated as the sum of a predominating macroscopic part (derived from the liquid-drop model of the atomic nucleus) and a microscopic part (derived from the nuclear shell model). By this way more accurate values for the binding energy are obtained than in the cases of using only the liquid drop model or the shell model. The shell correction energies of the ground-state of nuclei near closed shells are negative which results in further decreased values of the negative binding energy from the liquid drop model - and thus increased stability. An experimental signature for the shell-correction energy is obtained by subtracting a

calculated smooth macroscopic part from the measured total binding energy.

The shell-correction energy is plotted in Figure 8a using data from Reference 75. Two equally deep minima are obtained, one at Z = 108 and N = 162 for deformed nuclei with deformation parameters $\beta_2 \approx 0.22$, $\beta_4 \approx -0.07$ and the other one at Z = 114 and N = 184 for spherical SHEs. Different results are obtained from self-consistent Hartree-Fock-Bogoliubov calculations and relativistic mean-field models.[76, 77] They predict for spherical nuclei shells at Z = 114, 120 or 126 (indicated as dashed lines in Figure 8a) and N = 184 or 172.

The knowledge of ground-state binding energies, however, is not sufficient for the calculation of partial spontaneous fission half-lives. Here it is necessary to determine the size of the fission barrier over a wide range of deformation. The most accurate data were obtained for even-even nuclei using a macroscopic-microscopic model.[63] Partial spontaneous fission half-lives are plotted in Figure 8b. The landscape of fission half-lives reflects the landscape of shell-correction energies, because in the region of SHEs the height of the fission barrier is mainly determined by the ground-state shell correction energy, while the contribution from the macroscopic liquid-drop part approaches zero for Z = 104 and above. Nevertheless we see a significant increase of spontaneous fission half-life from 10^3 s for deformed nuclei to 10^{12} s for spherical SHEs. This difference originates from an increasing width of the fission barrier which becomes wider in the case of spherical nuclei.

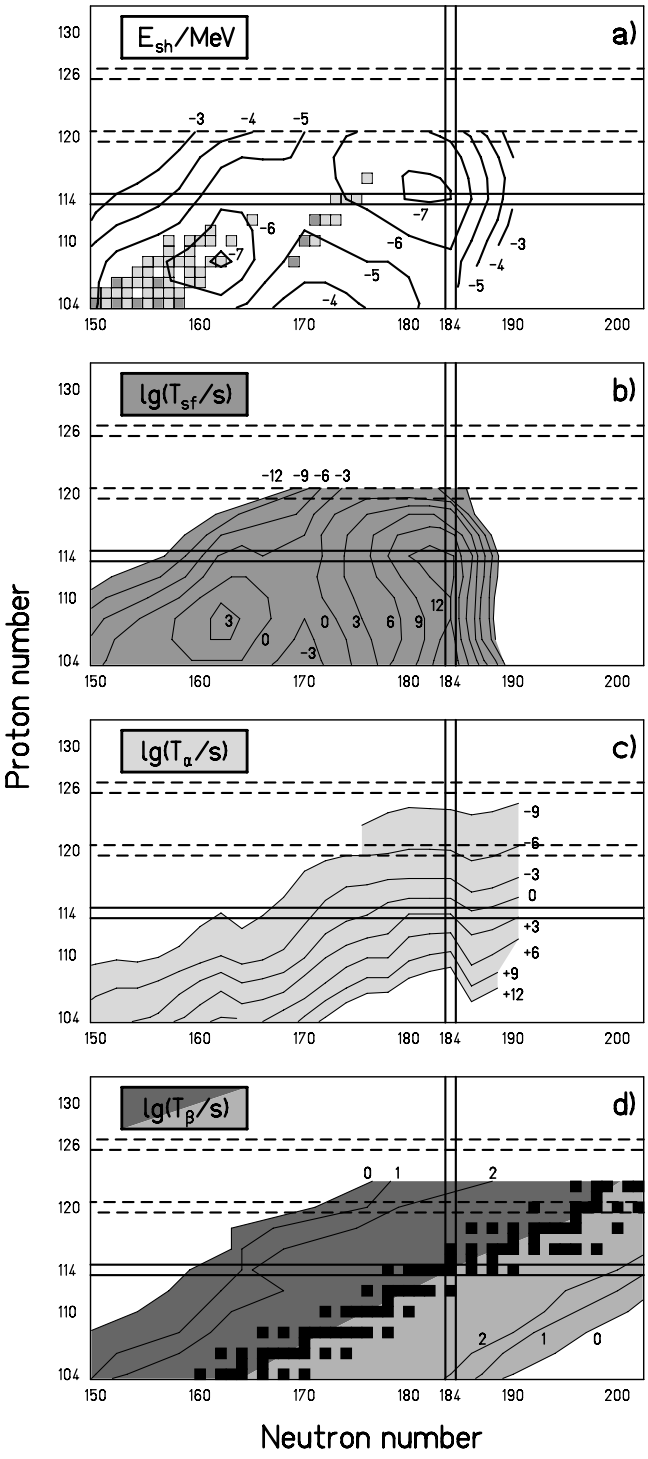

Figure 8. Shell-correction energy (a) and partial half-lives for spontaneous fission, α and β decay (b-d). The calculated values in (a) (c) are taken from References 63 and 75 and in (d) from Reference 78. The squares in (a) mark the nuclei presently known or under investigation, the filled squares in (d) mark the β stable nuclei.

Partial α half-lives decrease almost monotonically from 10^{12} s down to 10^{-9} s near Z = 126 (Figure 8c). The valley of β-stable nuclei passes through Z = 114, N = 184. At a distance of about 20 neutrons away from the bottom of this valley, β half-lives of isotopes have dropped down to values of one second[78] (Figure 8d).

Combining results from the individual decay modes one obtains the dominating partial half-life as shown in Figure 9 for even-even nuclei. The two regions of deformed heavy nuclei near N = 162 and spherical SHEs merge and form a region of α emitters surrounded by spontaneously fissioning nuclei. The longest half-lives are 1000 s for deformed heavy nuclei and 30 y for spherical SHEs. It is interesting to note that the longest half-lives are not reached for the doubly magic nucleus 114, but for Z = 110 and N = 182. This is a result of continuously increasing Q_α values with increasing atomic number. Therefore, α decay becomes the dominant decay mode beyond element 110 with continuously decreasing half-lives. For nuclei at N = 184 and Z < 110 half-lives are determined by β^- decay.

The four member α-decay chain of ^{292}116, the heaviest even-even nucleus, observed in the recent experiment in Dubna,[35] is also drawn in Figure 9. The arrows follow approximately the 1-s contour line down to ^{280}110. This is in agreement with the experimental observation. The nucleus ^{280}110 is predicted to decay by spontaneous fission. The average values of the measured half-lives of the nuclei along the decay chain, see sect. 3.2, are 53 ms – 2.6 s – 45 s – 7.6 s, respectively, which is about a factor of 10 longer than the calculated values. However, this deviation is well within the accuracy limits of the calculation. E.g., a change of the α energy of ^{288}114 by 350 keV only changes the half-life by a factor of 10. The decay chains of two other recently synthesized even-even nuclei, ^{270}110 [59] and ^{270}Hs,[41] are also drawn in the figure. In these cases the decay chains end by spontaneous fission at ^{262}Sg and ^{262}Rf, respectively.

For odd nuclei, partial α and spontaneous fission half-lives calculated by Smolanczuk and Sobiczewski[75] have to be multi-

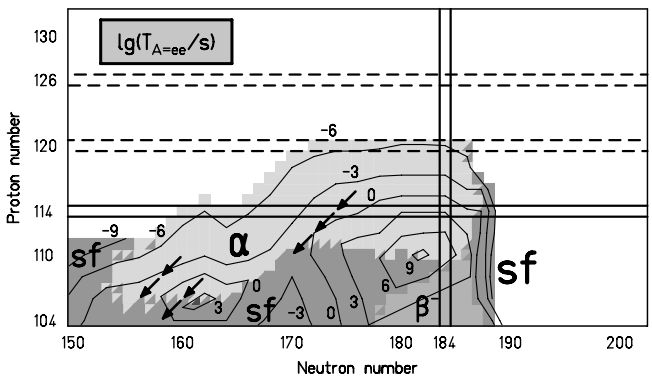

Figure 9. Dominant half-lives for α, β^+ decay/electron capture, β^- decay, and spontaneous fission. The data are valid for even-even nuclei only.

plied by a factor of 10 and 1000, respectively, thus making provisions for the odd particle hindrance factors. However, we have to keep in mind that fission hindrance factors show a wide distribution from 10^1 to 10^5, which is mainly a result of the specific levels occupied by the odd nucleon. For odd-odd nuclei, the fission hindrance factors from both the odd proton and the odd neutron are multiplied. For odd and odd-odd nuclei, the island character of α emitters disappears and for nuclei with neutron numbers 150 to 160 α-decay prevails down to rutherfordium and beyond. In the allegorical representation where the stability of SHEs is seen as an island in a sea of instability, even-even nuclei portray the situation at high-tide and odd nuclei at low-tide, when the island is connected to the mainland.

The interesting question arises, if and to which extent uncertainties related to the location of proton and neutron shell closures will change the half-lives of SHEs. Partial α and β half-lives are only insignificantly modified by shell effects, because their decay process occurs between neighboring nuclei. This is different for fission half-lives which are primarily determined by shell effects. However, the uncertainty related to the location of nuclei with the strongest shell-effects, and thus longest partial fission half-life at Z = 114, 120 or 126 and N = 172 or 184, is irrelevant concerning the longest 'total' half-life of SHEs. All regions for these SHEs are dominated by α decay. Alpha-decay half-lives will only be modified by a factor of up to approximately 100, if the double shell closure is not located at Z = 114 and N = 184. Only in the case of shell effects similar strong as in the double magic ^{208}Pb, the half-lives could become significantly shorter for nuclei above the shell closure and longer for the nuclei below.

The line of reasoning is, however, different concerning the production cross-section. The survival probability of the compound nucleus is determined among other factors significantly by the fission-barrier. Therefore, with respect to an efficient production yield, the knowledge of the location of minimal negative shell-correction energy is highly important. However, it may also turn out that shell effects in the region of SHEs are distributed across a number of subshell closures. In that case a wider region of less deep shell-correction energy would exist with corresponding modification of stability and production yield of SHEs.

5. Nuclear Reactions

The main features which determine the fusion process of heavy ions are (1) the fusion barrier and the related beam energy and excitation energy, (2) the ratio of surface tension versus Coulomb repulsion which determines the fusion probability and which strongly depends on the asymmetry of the reaction partners (the product Z_1Z_2 at fixed $Z_1 + Z_2$), (3) the impact parameter (centrality of collision) and related angular momentum, and (4) the ratio of neutron evaporation and of γ emission versus the fission of the compound nucleus.

In fusion reactions towards SHEs the product Z_1Z_2 reaches extremely large and the fission barrier extremely small values. In addition, the fission barrier itself is fragile, because it is solely built up from shell effects. For these reasons the fusion of SHEs is hampered twofold: (1) in the entrance channel by a high probability for re-separation and (2) in the exit channel by a high probability for fission. In contrast, the fusion of lighter elements proceeds unhindered through the contracting effect of the surface tension and the evaporation of neutrons instead of fission.

The effect of Coulomb repulsion on the cross-section starts to act severely for fusion reactions to produce elements beyond fermium. From there on a continuous decrease of cross-section was measured from microbarns for the synthesis of nobelium down to picobarns for the synthesis of element 112. Data obtained in reactions with ^{208}Pb and ^{209}Bi for the 1n-evaporation channel at low excitation energies of about 10–15 MeV (therefore named cold fusion) and in reactions with actinide targets at excitation energies of 35–45 MeV (hot fusion) for the 4n channel are plotted in Figure 10a and b, respectively.

Some features which the data reveal are pointed out in the following:

(1) So far no data were measured below cross-section values of about 0.5 pb. This is the limit presently set by experimental constraints. Considering the already long irradiation time of ≈1 month to reach a cross-section of 0.5 pb, it seems impractical to perform systematic studies on this cross-section level or even below. Further improvement of the experimental conditions is mandatory. Note in this context that the experimental sensitivity increased by three orders of magnitude since the 1982–83 search experiment for element 116 using a hot fusion reaction.[79]

(2) The cross-sections for elements lighter than 113 decrease by factors of 4 and 10 per element in the case of cold and hot fusion, respectively. The decrease is explained as a combined effect of increasing probability for re-separation of projectile and target nucleus and fission of the compound nucleus. Theoretical consideration and empirical descriptions, see e.g. References 17, 25, 80, and 81, suggest that the steep fall of cross-sections for cold fusion reactions may be strongly linked to increasing re-separation probability at high values of Z_1Z_2 while hot fusion cross-sections mainly drop because of strong fission losses at high excitation energies. Extremely small values result from an extrapolating these data into the

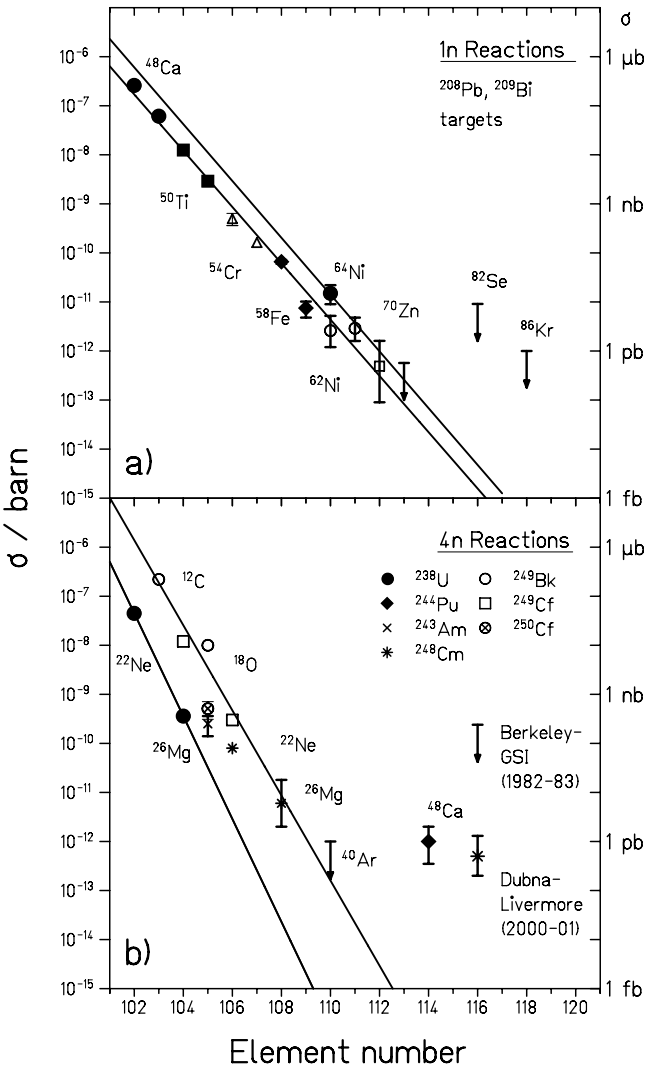

Figure 10. Measured cross-sections for reactions with ^{208}Pb and ^{209}Bi targets and 1n evaporation (a) and for reactions with actinide targets and 4n evaporation (b).

region of element 114 and beyond. However, strong shell effects for SHEs could lead to an increase of the fission barrier and thus to an increase of the survival probability of the compound nucleus, see also discussion in sect. 4. The relatively high values measured in Dubna for the synthesis of elements 114 and 116 would be in agreement with this argumentation. In the case of cold fusion only cross-section limits are known for the synthesis of elements 116 and 118.

(3) Locally an increase of the cross-section by a factor of 5.8 was measured for element 110 in cold fusion reactions when the beam was changed from ^{62}Ni to ^{64}Ni. It was speculated that this increase could be due to the increased value of the projectile neutron number. However, the assumption could not be confirmed in the case of element 112 which was synthesized using the most neutron rich stable zinc isotope with mass number 70.

A number of excitation functions were measured for the synthesis of elements from No to 110 using Pb and Bi targets.[17] For the even elements these data are shown together with the two data points measured for ^{278}112 in Figure 11. The maximum evaporation residue cross-section (1n channel) was measured at beam energies well below a one dimensional fusion barrier.[82] At the optimum beam energy projectile and target are just reaching the contact configuration in a central collision. The relatively simple fusion barrier based on the Bass model[82] is too high and a tunnelling process through this barrier cannot explain the measured cross-section. Various processes are possible, and are discussed in the literature, which result in a lowering of the fusion barrier. Among these processes transfer of nucleons and an excitation of vibrational degrees of freedom are the most important.[83, 84]

Target nuclei of actinide targets are strongly deformed and the height of the Coulomb barrier depends on the orientation of the deformation axes. The reaction ^{48}Ca + ^{248}Cm, studied in Dubna, was performed at a beam energy resulting in an excitation energy of approximately 34 MeV.[35] The observed decay chains were assigned to the 4n-evaporation channel. An excitation function which could provide experimental evidence for an orientation effect on the fusion cross-section is not yet measured.

It was pointed out in the literature[85] that closed shell projectiles and target nuclei are favorable synthesizing SHEs. The reason is not only a low (negative) reaction Q-value and thus a low excitation energy, but also that fusion of such systems is connected with a minimum of energy dissipation. The fusion path proceeds along cold fusion valleys, where the reaction partners maintain kinetic energy up to the closest possible distance. In this view the difference between cold and hot fusion is not only a result from gradually different values of excitation energy, but there exists a qualitative difference, which is on the one hand (cold fusion) based on a well ordered fusion process along paths of minimum dissipation of energy, and on the other hand (hot fusion) based on a process governed by the formation of a more or less energy equilibrated compound nucleus. The use of the double magic ^{48}Ca and actinide targets seems to proceed via an intermediate fusion process, possibly along a fusion valley less pronounced than in the case of cold fusion. Triggered by the recent experimental success of heavy element synthesis, a number of theoretical studies are in progress aiming to obtain a detailed understanding of the processes involved.[84, 86–91]

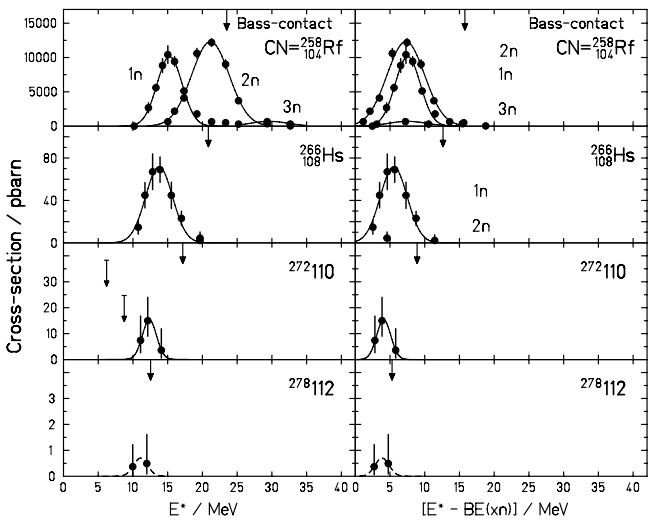

Figure 11. Measured even element excitation functions. On the left, the cross-sections are plotted as function of the dissipated energy E*, on the right, the neutron binding energies are subtracted.

Due to the great uncertainty concerning the influence of the various steps in the fusion of heavy elements, more and more precise experimental data are needed. It is especially important that various combinations of projectile and target be investigated, from very asymmetric systems to symmetric ones, and that excitation functions are measured. This provides information on how fast the cross-section decreases with increasing energy due to fission of the compound nucleus, and how fast cross-sections decrease on the low energy side due to the fusion barrier. From both slopes, information about the 'shape' of the fission and the fusion barriers can be obtained. At a high enough cross-section, these measurements can be complemented by in-beam γ-ray spectroscopy using the recoil-decay tagging method in order to study the influence of angular momentum on the fusion and survival probability.[92–94]

6. Summary and Outlook

The experimental work of the last two decades has shown that cross-sections for the synthesis of the heaviest elements decrease almost continuously. However, recent data on the synthesis of elements 114 and 116 in Dubna using hot fusion seem to break this trend when the region of spherical superheavy elements is reached. Therefore a confirmation is urgently needed that the region of spherical SHEs has finally been reached and that the exploration of the 'island' has started and can be performed even on a relatively high cross-section level.

The progress towards the exploration of the island of spherical SHEs is difficult to predict. However, despite the exciting new results, many questions of more general character are still awaiting an answer. New developments will not only make it possible to perform experiments aimed at synthesizing new elements in reasonable measuring times, but will also allow for a number of various other investigations covering reaction physics and spectroscopy.

One can hope that, during the coming years, more data will be measured in order to promote a better understanding of the stability of the heaviest elements and the processes that lead to fusion. A microscopic description of the fusion process will be needed for an effective explanation of all measured phenomena in the case of low dissipative energies. Then, the relationships between fusion probability and stability of the fusion products may also become apparent.

An opportunity for the continuation of experiments in the region of SHEs at decreasing cross-sections affords, among others, further accelerator developments. High current beams and radioactive beams are options for the future. At increased beam currents, values of tens of particle μA's may become accessible, the cross-section level for the performance of experiments can be shifted down into the region of tens of femtobarns, and excitation functions can be measured on the level of tenths of picobarns. High currents, in turn, call for the development of new targets and separator improvements. Radioactive ion beams, not as intense as the ones with stable isotopes, will allow for approaching the closed neutron shell *N*

= 184 already at lighter elements. The study of the fusion process using radioactive neutron rich beams will be highly interesting.

The half-lives of spherical SHEs are expected to be relatively long. Based on nuclear models, which are effective predictors of half-lives in the region of the heaviest elements, values from microseconds to years have been calculated for various isotopes. This wide range of half-lives encourages the application of a wide variety of experimental methods in the investigation of SHEs, from the safe identification of short lived isotopes by recoil-separation techniques to atomic physics experiments on trapped ions, and to the investigation of chemical properties of SHEs using long-lived isotopes.

References

(1) O. Hahn and F. Straßmann, Naturwissenschaften **27**, 11 (1939).
(2) L. Meitner and O.R. Frisch, Nature **143**, 239 (1939).
(3) G. Gamov, Proc. R. Soc. London A**126**, 632 (1930).
(4) C.F. von Weizsäcker, Z. Phys. **96**, 431 (1935).
(5) M. Göppert-Mayer, Phys. Rev. **74**, 235 (1948).
(6) O. Haxel, J.H.D. Jensen, and H.D. Suess, Phys. Rev. **75**, 1769 (1949).
(7) W.D. Myers and W.J. Swiatecki, Nucl. Phys. **81**, 1 (1966).
(8) H. Meldner, Ark. Fys. **36**, 593 (1967).
(9) S.G. Nilsson, J.R. Nix, A. Sobiczewski, Z. Szymanski, S. Wycech, C. Gustafson, and P. Möller, Nucl. Phys. A**115**, 545 (1968).
(10) U. Mosel and W. Greiner, Z. Phys. A**222**, 261 (1969).
(11) E.O. Fiset and J.R. Nix, Nucl. Phys. A**193**, 647 (1972).
(12) J. Randrup, S.E. Larsson, P. Möller, S.G. Nilsson, K. Pomorski, and A. Sobiczewski, Phys. Rev. C**13**, 229 (1976).
(13) W. Grimm, G. Herrmann, and H.-D. Schüssler, Phys. Rev. Lett. **26**, 1040 (1971).
(14) G.N. Flerov and G.M. Ter-Akopian, Rep. Prog. Phys. **46**, 817 (1983).
(15) G. Münzenberg, W. Faust, S. Hofmann, P. Armbruster, K. Güttner, and H. Ewald, Nucl. Instr. and Meth. **161**, 65 (1979).
(16) S. Hofmann, W. Faust, G. Münzenberg, W. Reisdorf, P. Armbruster, K. Güttner, and H. Ewald, Z. Phys. A**291**, 53 (1979).
(17) S. Hofmann and G. Münzenberg, Rev. Mod. Phys. **72**, 733 (2000).
(18) S. Hofmann, *On beyond uranium - Journey to the end of the Periodic Table*, Science Spectra Book Series, Vol. 2, Series edited by V. Moses, ISBN 0-415-28495-3 (Taylor and Francis, London and New York, 2002) pp. 216.
(19) M. Schädel, *The Chemistry of Superheavy Elements*, edited by M. Schädel ISBN 1-4020-1250-0 (Kluwer Academic Publishers, Dordrecht, 2003) pp. 300.
(20) P. Armbruster, J. Eidens, J.W. Grueter, H. Lawin, E. Roeckl, and K. Sistemich, Nucl. Instr. and Meth. **91**, 499 (1971).
(21) H. Folger, W. Hartmann, F.P. Heßberger, S. Hofmann, J. Klemm, G. Münzenberg, V. Ninov, W. Thalheimer, and P. Armbruster, Nucl. Instr. and Meth. A**362**, 64 (1995).
(22) S. Saro, R. Janik, S. Hofmann, H. Folger, F.P. Heßberger, V. Ninov, H.J. Schött, A.N. Andreyev, A.P. Kabachenko, A.G. Popeko, and A.V. Yeremin, Nucl. Instr. and Meth. A**381**, 520 (1996).
(23) S. Hofmann, F.P. Heßberger, D. Ackermann, G. Münzenberg, S. Antalic, P. Cagarda, B. Kindler, J. Kojouharova, M. Leino, B. Lommel, R, Mann, A.G. Popeko, S. Reshitko, S. Saro, J. Uusitalo, and A.V. Yeremin, Eur. Phys. J. A**14**, 147 (2002).
(24) G. Münzenberg, Rep. Prog. Phys. **51**, 57 (1988).
(25) S. Hofmann, Rep. Prog. Phys. **61**, 639 (1998).
(26) M. Schädel, J. Nucl. Radiochem. Sciences **3**, 113 (2002).
(27) S. Hofmann, V. Ninov, F.P. Heßberger, P. Armbruster, H. Folger, G. Münzenberg, H.J. Schött, A.G. Popeko, A.V. Yeremin, A.N. Andreyev, S. Saro, R. Janik, and M. Leino, Z. Phys. A**350**, 277 (1995).
(28) S. Hofmann, V. Ninov, F.P. Heßberger, P. Armbruster, H. Folger, G. Münzenberg, H.J. Schött, A.G. Popeko, A.V. Yeremin, S. Saro, R. Janik, and M. Leino, Z. Phys. A**354**, 229 (1996).
(29) S. Hofmann, V. Ninov, F.P. Heßberger, P. Armbruster, H. Folger, G. Münzenberg, H.J. Schött, A.G. Popeko, A.V. Yeremin, A.N. Andreyev, S. Saro, R. Janik, and M. Leino, Z. Phys. A**350**, 281 (1995).
(30) Yu.Ts. Oganessian, A.V. Yeremin, G.G. Gulbekian, S.L. Bogomolov, V.I. Chepigin, B.N. Gikal, V.A. Gorshkov, M.G. Itkis, A.P. Kabachenko, V.B. Kutner, A.Yu. Lavrentev, O.N. Malyshev, A.G. Popeko, J. Rohac, R.N. Sagaidak, S. Hofmann, G. Münzenberg, M. Veselsky, S. Saro, N. Iwasa, and K. Morita, Eur. Phys. J. A**5**, 63 (1999).
(31) Yu.Ts. Oganessian, A.V. Yeremin, A.G. Popeko, S.L. Bogomolov, G.V. Buklanov, M.L. Chelnokov, V.I. Chepigin, B.N. Gikal, V.A. Gorshkov, G.G. Gulbekian, M.G. Itkis, A.P. Kabachenko, A.Yu. Lavrentev, O.N. Malyshev, J. Rohac, R.N. Sagaidak, S. Hofmann, S. Saro, G. Giardina, and K. Morita, Nature **400**, 242 (1999).
(32) Yu.Ts. Oganessian, V.K. Utyonkov, Yu.V. Lobanov, F.Sh. Abdullin, A.N. Polyakov, I.V. Shirokovsky, Yu.S. Tsyganov, G.G. Gulbekian, S.L. Bogomolov, B.N. Gikal, A.N. Mezentsev, S. Iliev, V.G. Subbotin, A.M. Sukhov, G.V. Buklanov, K. Subotic, M.G. Itkis, K.J. Moody, J.F. Wild, N.J. Stoyer, M.A. Stoyer, and R.W. Lougheed, Phys. Rev. Lett. **83**, 3154 (1999).
(33) Yu.Ts. Oganessian, V.K. Utyonkov, Yu.V. Lobanov, F.Sh. Abdullin, A.N. Polyakov, I.V. Shirokovsky, Yu.S. Tsyganov, G.G. Gulbekian, S.L. Bogomolov, B.N. Gikal, A.N. Mezentsev, S. Iliev, V.G. Subbotin, A.M. Sukhov, O.V. Ivanov, G.V. Buklanov, K. Subotic, M.G. Itkis, K.J. Moody, J.F. Wild, N.J. Stoyer, M.A. Stoyer, and R.W. Lougheed, Phys. Rev. C**62**, 041604 (2000).
(34) Yu.Ts. Oganessian, V.K. Utyonkov, Yu.V. Lobanov, F.Sh. Abdullin, A.N. Polyakov, I.V. Shirokovsky, Yu.S. Tsyganov, G.G. Gulbekian, S.L. Bogomolov, B.N. Gikal, A.N. Mezentsev, S. Iliev, V.G. Subbotin, A.M. Sukhov, O.V. Ivanov, G.V. Buklanov, K. Subotic, M.G. Itkis, K.J. Moody, J.F. Wild, N.J. Stoyer, M.A. Stoyer, R.W. Lougheed, C.A. Laue, Ye.A. Karelin, and A.N. Tatarinov, Phys. Rev. C**63**, 011301 (2000).
(35) Yu.Ts. Oganessian, V.K. Utyonkov, and K.J. Moody, Physics of Atomic Nuclei **64**, 1349 (2001).
(36) Yu.A. Lazarev, Yu.V. Lobanov, Yu.Ts. Oganessian, V.K. Utyonkov, F.Sh. Abdullin, G.V. Buklanov, B.N. Gikal, S. Iliev, A.N. Mezentsev, A.N. Polyakov, I.M. Sedykh, I.V. Shirokovsky, V.G. Subbotin, A.M. Sukhov, Yu.S. Tsyganov, V.E. Zhuchko, R.W. Lougheed, K.J. Moody, J.F. Wild, E.K. Hulet, and J.H. McQuaid, Phys. Rev. Lett. **73**, 624 (1994).
(37) M. Schädel, W. Brüchle, R. Dressler, B. Eichler, H.W. Gäggeler, R. Günther, K.E. Gregorich, D.C. Hoffman, S. Hübener, D.T. Jost, J.V. Kratz, W. Paulus, D. Schumann, S. Timokhin, N. Trautmann, A. Türler, G. Wirth, and A. Yakuschev, Nature **388**, 55 (1997).
(38) A. Türler, W. Brüchle, R. Dressler, B. Eichler, R. Eichler, H.W. Gäggeler, M. Gärtner, J.-P. Glatz, K.E. Gregorich, S. Hübener, D.T. Jost, V.Ya. Lebedev, V.G. Pershina, M. Schädel, S. Taut, S.N. Timokhin, N. Trautmann, A. Vahle, and A.B. Yakushev, Angew. Chem. Int. Ed. **38**, 2212 (1999).

(39) P.A. Wilk, K.E. Gregorich, A. Türler, C.A. Laue, R. Eichler, V. Ninov, J.L. Adams, U.W. Kirbach, M.R. Lane, D.M. Lee, J.B. Patin, D.A. Shaughnessy, D.A. Strellis, H. Nitsche, and D.C. Hoffman, Phys. Rev Lett. **85**, 2697 (2000).

(40) R. Eichler, W. Brüchle, R. Dressler, Ch.E. Düllmann, B. Eichler, H.W. Gäggeler, K.E. Gregorich, D.C. Hoffman, S. Hübener, D.T. Jost, U.W. Kirbach, C.A. Laue, V.M. Lavanchy, H. Nitsche, J.B. Patin, D. Piquet, M. Schädel, D.A. Shaughnessy, D.A. Strellis, S. Taut, L. Tobler, Y.S. Tsyganov, A. Türler, A. Vahle, P.A. Wilk, and A.B. Yakushev, Nature **407**, 63 (2000).

(41) Ch.E. Düllmann, W. Brüchle, R. Dressler, K. Eberhardt, B. Eichler, R. Eichler, H.W. Gäggeler, T.N. Ginter, F. Glaus, K.E. Gregorich, D.C. Hoffman, E. Jäger, D.T. Jost, U.W. Kirbach, D.M. Lee, H. Nitsche, J.B. Patin, V. Pershina, D. Piguet, Z. Qin, M. Schädel, B. Schausten, E. Schimpf, H.-J. Schött, S. Soverna, R. Sudowe, P. Thörle, S.N. Timokhin, N. Trautmann, A. Türler, A. Vahle, G. Wirth, A.B. Yakushev, and P.M. Zielinski, Nature **418**, 859 (2002).

(42) G. Münzenberg, S. Hofmann, F.P. Heßberger, W. Reisdorf, K.-H. Schmidt, J.H.R. Schneider, P. Armbruster, C.C. Sahm, and B. Thuma, Z. Phys. A**300**, 107 (1981).

(43) G. Münzenberg, P. Armbruster, S. Hofmann, F.P. Heßberger, H. Folger, J.G. Keller, V. Ninov, K. Poppensieker, A.B. Quint, W. Reisdorf, K.-H. Schmidt, J.R.H. Schneider, H.-J. Schött, K. Sümmerer, I. Zychor, M.E. Leino, D. Ackermann, U. Gollerthan, E. Hanelt, W. Morawek, D. Vermeulen, Y. Fujita, and T. Schwab, Z. Phys. A**333**, 163 (1989).

(44) S. Hofmann, F.P. Heßberger, V. Ninov, P. Armbruster, G. Münzenberg, C. Stodel, A.G. Popeko, A.V. Yeremin, S. Saro, and M. Leino, Z. Phys. A**358**, 377 (1997).

(45) G. Münzenberg, P. Armbruster, H. Folger, F.P. Heßberger, S. Hofmann, J. Keller, K. Poppensieker, W. Reisdorf, K.H. Schmidt, H.J. Schött, M.E. Leino, and R. Hingmann, Z. Phys. A**317**, 235 (1984).

(46) G. Münzenberg, P. Armbruster, G. Berthes, H. Folger, F.P. Heßberger, S. Hofmann, K. Poppensieker, W. Reisdorf, B. Quint, K.H. Schmidt, H.J. Schött, K. Sümmerer, I. Zychor, M. Leino, U. Gollerthan, and E. Hanelt, Z. Phys. A**324**, 489 (1986).

(47) G. Münzenberg, P. Armbruster, F.P. Heßberger, S. Hofmann, K. Poppensieker, W. Reisdorf, J.R.H. Schneider, W.F.W. Schneider, K.H. Schmidt, C.C. Sahm, and D. Vermeulen, Z. Phys. A**309**, 89 (1982).

(48) G. Münzenberg, W. Reisdorf, S. Hofmann, Y.K. Agarwal, F.P. Heßberger, K. Poppensieker, J.R.H. Schneider, W.F.W. Schneider, K.H. Schmidt, H.J. Schött, P. Armbruster, C.C. Sahm, and D. Vermeulen, Z. Phys. A**315**, 145 (1984).

(49) G. Münzenberg, S. Hofmann, F.P. Heßberger, H. Folger, V. Ninov, K. Poppensieker, B. Quint, W. Reisdorf, H.J. Schött, K. Sümmerer, P. Armbruster, M.E. Leino, D. Ackermann, U. Gollerthan, E. Hanelt, W. Morawek, Y. Fujita, T. Schwab, and A. Türler, Z. Phys. A**330**, 435 (1988).

(50) Yu.A. Lazarev, Yu.V. Lobanov, Yu.Ts. Oganessian, Yu.S. Tsyganov, V.K. Utyonkov, F.Sh. Abdullin, S. Iliev, A.N. Polyakov, J. Rigol, I.V. Shirokovsky, V.G. Subbotin, A.M. Sukhov, G.V. Buklanov, B.N. Gikal, V.B. Kutner, A.N. Mezentsev, I.M. Sedykh, D.V. Vakatov, R.W. Lougheed, J.F. Wild, K.J. Moody, and E.K. Hulet, Phys. Rev. Lett. **75**, 1903 (1995).

(51) A. Ghiorso, J.M. Nitschke, J.R. Alonso, C.T. Alonso, M. Nurmia, G.T. Seaborg, E.K. Hulet, and R.W. Lougheed, Phys. Rev. Lett. **33**, 1490 (1974).

(52) M.R. Schmorak, Nuclear Data Sheets **59**, 507 (1990).

(53) K. Morita, K. Morimoto, D. Kaji, A. Yoneda, A. Yoshida, T. Suda, E. Ideguchi, T. Ohnishi, Y.-L. Zhao, H. Xu, T. Zheng, H. Haba, H. Kudo, K. Sueki, A. Ozawa, F. Tokanai, H. Koura, R. Kanungo, K. Katori, and I. Tanihata, RIKEN Accel. Prog. Rep. **35**, 90 (2003).

(54) K. Morita, K. Morimoto, D. Kaji, A. Yoneda, A. Yoshida, T. Suda, E. Ideguchi, T. Ohnishi, Y.-L. Zhao, H. Xu, T. Zheng, H. Haba, H. Kudo, K. Sueki, A. Ozawa, F. Tokanai, H. Koura, A.V. Yeremin, R. Kanungo, K. Katori, and I. Tanihata, RIKEN Accel. Prog. Rep. **35**, 91 (2003).

(55) S. Ćwiok, S. Hofmann, and W. Nazarewicz, Nucl. Phys. A**573**, 356 (1994).

(56) T.N. Ginter, *Proceedings of the Third International Conference on Fission and Properties of Neutron-Rich Nuclei*, Sanibel Island, Florida, November 3-9, 2002, to be published.

(57) A. Ghiorso, D. Lee, L.P. Sommerville, W. Loveland, J.M. Nitschke, W. Ghiorso, G.T. Seaborg, P. Wilmarth, R. Leres, A. Wydler, M. Nurmia, K. Gregorich, K. Czerwinski, R. Gaylord, T. Hamilton, N.J. Hannink, D.C. Hoffman, C. Jarzynski, C. Kacher, B. Kadkhodayan, S. Kreek, M. Lane, A. Lyon, M.A. McMahan, M. Neu, T. Sikkeland, W.J. Swiatecki, A. Türler, J.T. Walton, and S. Yashita, Phys. Rev. C**51**, R2293 (1995).

(58) Yu.A. Lazarev, Yu.V. Lobanov, Yu.Ts. Oganessian, V.K. Utyonkov, F.Sh. Abdullin, A.N. Polyakov, J. Rigol, I.V. Shirokovsky, Yu.S. Tsyganov, S. Iliev, V.G. Subbotin, A.M. Sukhov, G.V. Buklanov, B.N. Gikal, V.B. Kutner, A.N. Mezentsev, K. Subotic, J.F. Wild, R.W. Lougheed, and K.J. Moody, Phys. Rev. C**54**, 620 (1996).

(59) S. Hofmann, F.P. Heßberger, D. Ackermann, S. Antalic, P. Cagarda, S. Ćwiok, B. Kindler, J. Kojouharova, B. Lommel, R. Mann, G. Münzenberg, A.G. Popeko, S. Saro, H.J. Schött, and A.V. Yeremin, Eur. Phys. J. A**10**, 5 (2001).

(60) S. Ćwiok, W. Nazarewicz, and P.H. Heenen, Phys. Rev. Lett. **83**, 1108 (1999).

(61) I. Muntian, Z. Patyk, and A. Sobiczewski, Phys. Rev. C**60**, 041302 (1999).

(62) R. Smolanczuk, Phys. Rev. Lett. **83**, 4705 (1999).

(63) R. Smolanczuk, J. Skalski, and A. Sobiczewski, Phys. Rev. C**52**, 1871 (1995).

(64) V. Ninov, K.E. Gregorich, W. Loveland, A. Ghiorso, D.C. Hoffman, D.M. Lee, H. Nitsche, W.J. Swiatecki, U.W. Kirbach, C.A. Laue, J.L. Adams, J.B. Patin, D.A. Shaughnessy, D.A. Strellis, and P.A. Wilk, Phys. Rev. Lett. **83**, 1104 (1999).

(65) C. Stodel, N. Alamanos, N. Amar, J.C. Angélique, R. Anne, G. Auger, J.M. Casandjian, R. Dayras, A. Drouart, J.M. Fontbonne, A. Gillibert, S. Grévy, D. Guerreau, F. Hanappe, R. Hue, A.S. Lalleman, N. Lecesne, T. Legou, M. Lewitowicz, R. Lichtenthäler, E. Liénard, L. Maunoury, W. Mittig, N. Orr, J. Péter, E. Plagnol, G. Politi, M.G. Saint-Laurant, J.C. Steckmeyer, J. Tillier, R. de Tourreil, A.C.C. Villari, J.P. Wieleczko, and A. Wieloch, *Proceedings of the Tours Symposium on Nuclear Physics IV*, edited by M. Arnould et al., AIP Conference Proceedings 561 (AIP, New York, 2001) p. 344.

(66) K. Morimoto, K. Morita, I. Tanihata, N. Iwasa, R. Kanungo, T. Kato, K. Katori, H. Kudo, T. Suda, I. Sugai, S. Takeuchi, F. Tokanai, K. Uchiyama, Y. Wakasaya, T. Yamaguchi, A. Yeremin, A. Yoneda, and A. Yoshida, *Proceedings of the Tours Symposium on Nuclear Physics IV*, edited by M. Arnould et al., AIP Conference Proceedings 561 (AIP, New York, 2001) p. 354.

(67) V. Ninov, K.E. Gregorich, W. Loveland, A. Ghiorso, D.C. Hoffman, D.M. Lee, H. Nitsche, W.J. Swiatecki, U.W. Kirbach, C.A. Laue, J.L. Adams, J.B. Patin, D.A. Shaughnessy, D.A. Strellis, and P.A. Wilk, Phys. Rev.

Lett. **89**, 039901 (2002).
(68) V.B. Kutner, S.L. Bogomolov, G.G. Gulbekian, A.A. Efremov, G.N. Ivanov, A.N. Lebedev, V.Ya. Lebedev, V.N. Loginov, Yu.Ts. Oganessian, A.B. Yakushev, and N.Yu. Yazvitsky, *Proceedings of the 15th International Conference on Cyclotrons and their Applications*, edited by E. Baron and M. Lieuvin (IOP, Bristol, 1998), p. 405.
(69) A.V. Yeremin, A.N. Andreyev, D.D. Bogdanov, G.M. Ter-Akopian, V.I. Chepigin, V.A. Gorshkov, A.P. Kabachenko, O.N. Malyshev, A.G. Popeko, R.N. Sagaidak, S. Sharo, E.N. Voronkov, A.V. Taranenko, and A.Yu. Lavrentjev, Nucl. Instr. and Meth. A**350**, 608 (1994).
(70) A.V. Yeremin, D.D. Bogdanov, V.I. Chepigin, V.A. Gorshkov, A.P. Kabachenko, O.N. Malyshev, A.G. Popeko, R.N. Sagaidak, A.Yu. Ter-Akopian, and A.Yu. Lavrentjev, Nucl. Instr. and Meth. B**126**, 329 (1997).
(71) Yu.A. Lazarev, Yu.V. Lobanov, A.N. Mezentsev, Yu.Ts. Oganessian, V.G. Subbotin, V.K. Utyonkov, F.Sh. Abdullin, V.V. Bechterev, S. Iliev, I.V. Kolesov, A.N. Polyakov, I.M. Sedykh, I.V. Shirokovsky, A.M. Sukhov, Yu.S. Tsyganov, and V.E. Zhuchko, *Proceedings of the International School Seminar on Heavy Ion Physics*, edited by Yu.Ts. Oganessian et al. (Joint Institute for Nuclear Research, Dubna, 1993), Vol. II, p. 497.
(72) B. Kadkhodayan, A. Türler, K.E. Gregorich, P.A. Baisden, K.R. Czerwinski, B. Eichler, H.W. Gäggeler, T.M. Hamilton, D.T. Jost, C.D. Kacher, A. Kovacs, S.A. Kreek, M.R. Lane, M. Mohar, M.P. Neu, N.J. Stoyer, E.R. Sylwester, M.D. Lee, M.J. Nurmia, G.T. Seaborg, and D.C. Hoffman, Radiochim. Acta **72**, 169 (1996).
(73) J.V. Kratz, M.K. Gober, H.P. Zimmermann, M. Schädel, W. Brüchle, E. Schimpf, K.E. Gregorich, A. Türler, N.J. Hannink, K.R. Czerwinski, B. Kadkhodayan, D.M. Lee, M.J. Nurmia, D.C. Hoffman, H. Gäggeler, D. Jost, J. Kovacs, U.W. Scherer, and A. Weber, Phys. Rev. C**45**, 1064 (1992).
(74) A. Türler, R. Dressler, B. Eichler, H.W. Gäggeler, D.T. Jost, M. Schädel, W. Brüchle, K.E. Gregorich, N. Trautmann, and S. Taut, Phys. Rev. C**57**, 1648 (1998).
(75) R. Smolanczuk and A. Sobiczewski, *Proceedings of the XV. Nuclear Physics Divisional Conference on Low Energy Nuclear Dynamics*, edited by Yu.Ts. Oganessian et al. (World Scientific, Singapore, 1995), p. 313.
(76) S. Ćwiok, J. Dobaczewski, P.H. Heenen, P. Magierski, and W. Nazarewicz, Nucl. Phys. A**611**, 211 (1996).
(77) K. Rutz, M. Bender, T. Bürvenich, T. Schilling, P.G. Reinhard, J.A. Maruhn, and W. Greiner, Phys. Rev. C**56**, 238 (1997).
(78) P. Möller, J.R. Nix, and K.L. Kratz, Atomic Data and Nucl. Data Tables **66**, 131 (1997).
(79) P. Armbruster, Y.K. Agarwal, W. Brüchle, M. Brügger, J.P. Dufour, H. Gäggeler, F.P. Heßberger, S. Hofmann, P. Lemmertz, G. Münzenberg, K. Poppensieker, W. Reisdorf, M. Schädel, K.-H. Schmidt, J.R.H. Schneider, W.F.W. Schneider, K. Sümmerer, D. Vermeulen, G. Wirth, A. Ghiorso, K.E. Gregorich, D. Lee, M. Leino, K.J. Moody, G.T. Seaborg, R.B. Welch, P. Wilmarth, S. Yashita, C. Frink, N. Greulich, G. Herrmann, U. Hickmann, N. Hildebrand, J.V. Kratz, N. Trautmann, M.M. Fowler, D.C. Hoffman, W.R. Daniels, H.R. von Gunten, and H. Dornhöfer, Phys. Rev. Lett. **54**, 406 (1985).
(80) W. Reisdorf and M. Schädel, Z. Phys. A**343**, 47 (1992).
(81) M. Schädel and S. Hofmann, J. Radioanal. Nucl. Chem. **203**, 283 (1996).
(82) R. Bass, Nucl. Phys. A**231**, 45 (1974).
(83) W. von Oertzen, Z. Phys. A**342**, 177 (1992).
(84) V.Yu. Denisov and S. Hofmann, Phys. Rev. C**61**, 034606 (2000).
(85) R.K. Gupta, C. Parvulescu, A. Sandulescu, and W. Greiner, Z. Phys. A**283**, 217 (1977).
(86) V.Yu. Denisov and W. Nörenberg, Eur. Phys. J. A**15**, 375 (2002).
(87) Y. Aritomo, T. Wada, M. Ohta, and Y. Abe, Phys. Rev. C**59**, 796 (1999).
(88) V.I. Zagrebaev, Phys. Rev. C**64**, 034606 (2001).
(89) G. Giardina, S. Hofmann, A.I. Muminov, and A.K. Nasirov, Eur. Phys. J. A**8**, 205 (2000).
(90) R. Smolanczuk, Phys. Rev. C**63**, 044607 (2001).
(91) G.G. Adamian, N.V. Antonenko, and W. Scheid, Nucl. Phys. A**678**, 24 (2000).
(92) P. Reiter, T.L. Khoo, C.J. Lister, D. Seweryniak, I. Ahmad, M. Alcorta, M.P. Carpenter, J.A. Cizewski, C.N. Davids, G. Gervais, J.P. Greene, W.F. Henning, R.V.F. Janssens, T. Lauritsen, S. Siem, A.A. Sonzogni, D. Sullivan, J. Uusitalo, I. Wiedenhöver, N. Amzal, P.A. Butler, A.J. Chewter, K.Y. Ding, N. Fotiades, J.D. Fox, P.T. Greenlees, R.D. Herzberg, G.D. Jones, W. Korten, M. Leino, and K. Vetter, Phys. Rev. Lett. **82**, 509 (1999).
(93) P. Reiter, T.L. Khoo, T. Lauritsen, C.J. Lister, D. Seweryniak, A.A. Sonzogni, I. Ahmad, N. Amzal, P. Bhattacharyya, P.A. Butler, M.P. Carpenter, A.J. Chewter, J.A. Cizewski, C.N. Davids, K.Y. Ding, N. Fotiades, J.P. Greene, P.T. Greenlees, A. Heinz, W.F. Henning, R.-D. Herzberg, R.V.F. Janssens, G.D. Jones, H. Kankaanpää, F.G. Kondev, W. Korten, M. Leino, S. Siem, J. Uusitalo, K. Vetter, and I. Wiedenhöver, Phys. Rev. Lett. **84**, 3542 (2000).
(94) R.-D. Herzberg, N. Amzal, F. Becker, P.A. Butler, A.J.C. Chewter, J.F.C. Cocks, O. Dorvaux, K. Eskola, J. Gerl, P.T. Greenlees, N.J. Hammond, K. Hauschild, K. Helariutta, F. Heßberger, M. Houry, G.D. Jones, P.M. Jones, R. Julin, S. Juutinen, H. Kankaanpää, H. Kettunen, T.L. Khoo, W. Korten, P. Kuusiniemi, Y. Le Coz, M. Leino, C.J. Lister, R. Lucas, M. Muikku, P. Nieminen, R.D. Page, P. Rahkila, P. Reiter, Ch. Schlegel, C. Scholey, O. Stezowski, Ch. Theisen, W.H. Trzaska, J. Uusitalo, and H.J. Wollersheim, Phys. Rev. C**65**, 014303 (2001).